NUCLEAR STRUCTURE -- THEORY

PARITY INVERSION IN THE N=7 ISOTONES AND THE PAIRING BLOCKING EFFECT

H. Sagawa[a], B. A. Brown, and H. Esbensen[c]

The essential mechanism which causes the parity inversion in ^{11}Be has been a long-standing open question [1]: the $J^\pi = \frac{1}{2}^+$ state is the ground state of ^{11}Be, while the naive shell-model would predict a $J^\pi = \frac{1}{2}^-$ state as the ground state of this odd-even 1p-shell nucleus. Although many large-basis shell-model calculations [2-6] have been carried out, they do not all reproduce the parity inversion. For those calculations that do reproduce the inversion [5-7], it is important to go beyond just the numerical results and to understand the qualitative physical mechanisms responsible. In this letter we explore this issue from the weak coupling picture of the core and valence particle. The validity of this model is discussed in comparison with realistic shell model wave functions. We also study how these mechanisms affect other odd-even N=7 isotones, in particular ^{9}He. The shell-model calculations are performed by using the recent Warburton-Brown effective interaction [7]. This new interaction was obtained from a least squares fit of single-particle energies, two-body matrix elements and two-body interaction potential strengths to 51 1p shell data and 165 1p-1d2s (cross shell) data on binding energies and excitation energies in nuclei with A=10-22. The rms deviation between the theoretical and experimental energies was about 330 keV. This interaction represents a significant improvement over the Millener-Kurath interaction [3] in many ways, but most importantly for this work, in its ability to accommodate a realistic N and Z dependence of the single-particle energies over a wide range of nuclei.

In the early 1960s, Talmi and Unna first noticed the parity inversion problem in ^{11}Be [1] and suggested that the proton-neutron monopole interaction in the mean field was the main cause. We have performed Hartree-Fock (H-F) calculations for the N=7 isotones to study the effect of the proton-neutron interaction in the mean field spectra. The H-F results in fig. 1 are obtained by using a Skyrme force SGII [10], and the particles are assumed to occupy the lowest single-particle orbits in the H-F potential in order. One observes large changes in the single-particle energies of the 1p- and 2s1d-shell orbits when one decreases the proton numbers. This is due to shallower neutron potential for smaller N=7 nuclei, and the neutron-proton interaction is responsible for this change. Notice also the inversion of $2s_{1/2}$ and $1d_{5/2}$ orbits which is caused by a smaller kinetic energy for the loosely-bound $2s_{1/2}$ than that of $1d_{5/2}$. However, the energy gap between the $2s_{1/2}$- and $1p_{1/2}$-state is still larger than 5 MeV and the proton-neutron monopole interaction is thus not enough to explain the parity inversion.

We note that this 5 MeV is the energy difference of the $2s_{1/2}$ single-particle state and the $1p_{1/2}$ single-hole state of "^{12}Be", where by "^{12}Be" we mean the semi-closed 1p-shell configuration for this nucleus. The corrections which remain to be considered are just the 1p shell proton pairing for the $1p_{1/2}$ state. But for the $2s_{1/2}$ state we need to consider in addition the effect of removing two neutron holes which leads to contributions from (1) the quadrupole collectivity of ^{10}Be, (2) the 1p-shell neutron pairing, and (3) the change in monopole interaction. It turns out with the Warburton-Brown interaction that (3) can be ignored. We will now discuss the contributions from (1) and (2).

A large deformation can also give an inverted spectra of the positive and negative parity states: the positive parity state with the asymptotic quantum number $[Nn_3\Lambda\Omega]$ =[220 1/2] comes lower in energy than the negative parity state [101 1/2] near the quadrupole deformation $\beta_2 \simeq 0.7$ in the deformed Nilsson diagram [11]. These states trace back to $1d_{5/2}$- and $1p_{1/2}$- states, respectively, in the spherical limit. Ragnarson et al.[12], performed cranking shell-model calculations with these Nilsson wave functions. In their calculations with different cranking Hamiltonians, the $5/2^+$ state came lower in energy than or at most about the same energy

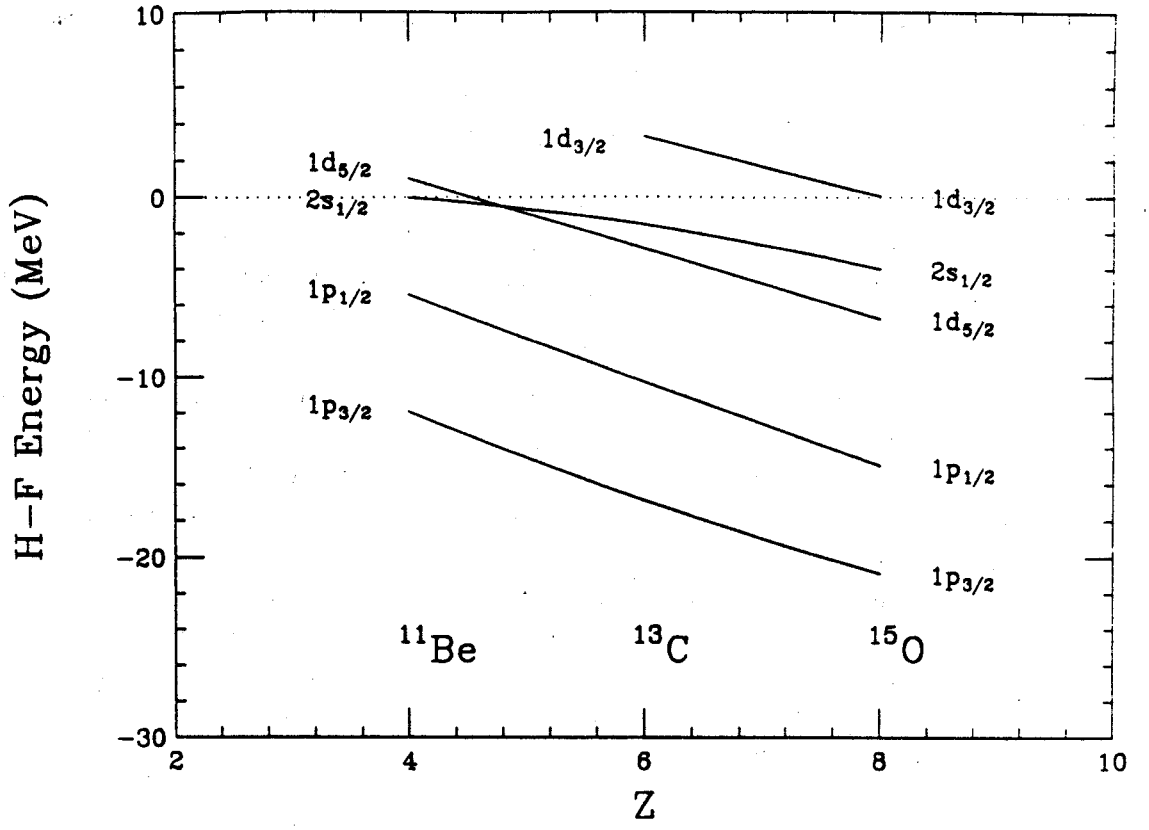

Figure 1: H-F single particle energies for the N=7 isotones calculated with a Skyrme interaction SGII.

as the $\frac{1}{2}^+$ state. This is due to the fact that the deformed Nilsson wave function with the asymptotic quantum number $[Nn_3\Lambda\Omega]$ =[220 1/2] at $\beta_2 \simeq 0.7$ is 80% $1d_{5/2}$, and the $2s_{1/2}$-state is a small component. Since the $\frac{5}{2}^+$-state must be an excited state with $E_x \geq 1.7$ MeV in the experiment, a large deformation is unlikely in the ground state of ^{11}Be . It has also been pointed out that a large deformation can not explain the experimental data for the total reaction cross sections of ^{11}Be both at high and medium energy energy heavy ion experiments [13]. This is due to the fact that the dominant $1d_{5/2}$-wave function in the Nilsson [220 1/2] state does not have a large halo due to the centrifugal barrier.

Although a large deformation in the intrinsic frame is unlikely, the 2^+ core excitation coupled with $1d_{5/2}$-state is an important component in the lowest $\frac{1}{2}^+$ shell-model state in ^{11}Be. We will now estimate the effect of the mixing of the core excitation. The $\frac{1}{2}^+$ ground state of ^{11}Be can be expressed approximately as [14]

$$\mid 1/2^+\rangle = \alpha_s \mid 2s_{\frac{1}{2}} \times 0^+\rangle + \alpha_d \mid 1d_{\frac{5}{2}} \times 2^+\rangle \qquad (1)$$

where 0^+ and 2^+ are the ground state and the first excited state at Ex=3.37 MeV in ^{10}Be and α_d will be calculated in perturbation theory. The single-particle energy of $1d_{5/2}$-state is $1 \simeq 2$ Mev higher that that of $2s_{1/2}$-state in the H-F calculations, and thus the total energy denominator for α_d is about 5 MeV. The coupling matrix element $\langle 2s_{1/2} \times 0^+ \mid V_{coup} \mid 1d_{5/2} \times 2^+\rangle$ is proportional to the transition amplitude of the core excitation in the particle-vibration coupling model [15]. Using the experimental transition strength from the ground state to the 2^+ state in ^{10}Be which is several times larger than the single-particle unit, the coupling matrix element is estimated to be 2.7 MeV. Thus $\alpha_d^2 \sim 0.20$ and the energy of the ground state is lowered by about 1.5 MeV. This estimate is consistent with the full shell-model calculation as well as the fact that the ^{10}Be to ^{11}Be $2s_{1/2}$ spectroscopic factor is large. We note, however, that the most direct test of the α_d^2 component will come from a

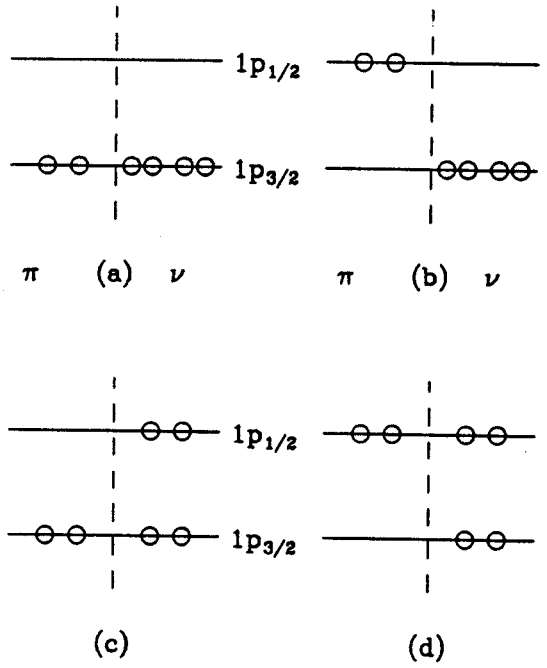

Figure 2: Pairing configurations for the ^{10}Be core. All configurations contribute to the pairing correlation for the $\frac{1}{2}^+$ state, while only two configurations (a) and (b) contribute for the $\frac{1}{2}^-$ state.

measurement of the ^{11}Be to ^{10}Be 2^+ $1d_{5/2}$ spectroscopic factor using a radioactive beam.

Finally, we will discuss the effect of the pairing correlations. The specific issue we address is the Pauli blocking effect due to the presence of the last neutron in N=7 isotones. Suppose the dominant configuration of the ground state is $2s_{1/2}$ and the first excited state is $1p_{1/2}$ which is the case in ^{11}Be. There are 4 available pairing configurations in the 1p-shell orbits for the ground state in ^{10}Be as is shown in fig. 2. The configurations (a) and (b) are available for both the positive and the negative parity states. On the other hand, the configurations (c) and (d) contribute to the positive parity state, but not to the negative parity state because of the Pauli blocking effect due to the presence of one additional neutron in the $1p_{1/2}$-orbit. This difference makes a substantial effect on the off-diagonal pairing matrix element as we will now show. We note that even though the diagrams in Fig. 2 are based upon a ^{10}Be core, we only use this core with respect to an evaluation of the pairing and quadrupole contributions, and, as mentioned above, the single-particle energy themselves are with respect to a ^{12}Be core.

Let us now study the pairing correlations quantitatively by using more realistic shell model wave functions. We expand the even-even core part of shell-model wave function as

$$\mid i\rangle = \sum_{\alpha=a,b,c,d} C(i,\alpha) \mid \alpha\rangle \tag{2}$$

where $C(i,\alpha)$ is the shell-model amplitude for each configuration. The wave functions are calculated with a full $0\hbar\omega$-configuration space for negative parity states and a full $1\hbar\omega$-configuration space for positive parity states by using the same effective interaction [7]. The pairing matrix element for the $\frac{1}{2}^-$ state is

$$\begin{aligned}\langle 1/2^- \mid V_{pair} \mid 1/2^-\rangle &= C(1/2^-,a)^2\langle a \mid V_{pair} \mid a\rangle + C(1/2^-,b)^2\langle b \mid V_{pair} \mid b\rangle \\ &+ 2\times C(1/2^-,a)C(1/2^-,b)\langle a \mid V_{pair} \mid b\rangle \end{aligned} \tag{3}$$

There is only one cross term in eq. (3). The matrix element for the positive parity state has more terms:

$$\begin{aligned}\langle 1/2^+ \mid V_{pair} \mid 1/2^+\rangle = C(1/2^+,a)^2\langle a \mid V_{pair} \mid a\rangle + C(1/2^+,b)^2\langle b \mid V_{pair} \mid b\rangle \\ +C(1/2^+,c)^2\langle c \mid V_{pair} \mid c\rangle + C(1/2^+,d)^2\langle d \mid V_{pair} \mid d\rangle \\ +2\times C(1/2^+,a)C(1/2^+,b)\langle a \mid V_{pair} \mid b\rangle + 2\times C(1/2^+,a)C(1/2^+,c)\langle a \mid V_{pair} \mid c\rangle \\ +2\times C(1/2^+,b)C(1/2^+,d)\langle b \mid V_{pair} \mid d\rangle + 2\times C(1/2^+,c)C(1/2^+,d)\langle c \mid V_{pair} \mid d\rangle \end{aligned} \quad (4)$$

The two-body pairing matrix elements for 1p-shell nuclei are $\langle (p_{3/2})^2 \mid V_{pair} \mid (p_{3/2})^2\rangle = -3.85$ MeV, $\langle (p_{3/2})^2 \mid V_{pair} \mid (p_{1/2})^2\rangle = -3.84$ MeV and $\langle (p_{1/2})^2 \mid V_{pair} \mid (p_{1/2})^2\rangle = -1.22$ MeV for the present calculations [7]. The pairing energy difference between the two states is found to be large:

$$\begin{aligned}\Delta E_{pair} &= \langle 1/2^- \mid V_{pair} \mid 1/2^-\rangle - \langle 1/2^+ \mid V_{pair} \mid 1/2^+\rangle \\ &= 2.19 \text{ MeV}\end{aligned} \quad (5)$$

The 5 MeV energy difference between the $2s_{1/2}$ and the $1p_{1/2}$ states in the mean field, as shown in fig.1, is thus effectively reduced to about zero by a combination of the core excitation and the Pauli blocking effects. The blocking effect exists also for other N=7 nuclei. In ^{9}He, the value ΔE_{pair} is 3.28 MeV which could result in another inverted spectrum in this nucleus. The value of ΔE_{pair} in ^{13}C is 2.42 MeV which is not enough to make the parity inversion because of the larger single-particle energy gap, and a somewhat smaller effect of the 2^+ core excitation compared to ^{11}Be.

In summary, we have studied the possible mechanisms for the parity inversion spectrum of ^{11}Be. We have pointed out that the core excitation to the first 2^+-state and the pairing blocking effect are both important to produce the parity inversion. The proton-neutron monopole interaction in the mean field is significant, but not enough to make the inverted spectra as is shown in fig. 1. Our study suggests a possible parity inversion also in ^{9}He. The combined effects of 2^+ core excitation and Pauli blocking are important for reducing the excitation energy of "core excited" states of nuclei in a wide region of the mass table [17,18]. However, it is only when these are combined with the reduced single-particle spacing, which occurs for the loosely bound states in nuclei far from stability, that the peculiar feature of "parity inversion" and "islands of inversion" occur.

The features we have discussed here for the N=7 isotones have interesting implications for other nuclei in this mass region near the neutron-drip. For example, the Warburton-Brown interaction [7] predicts that the configurations with two-neutrons excited from the 1p to the 1d2s shell are degenerate with the 1p shell configuration for ^{12}Be and ^{11}Li because of the same physical reasons described in this manuscript. It will be important in future theoretical investigations to explore the consequences of the mixing between these 1p and 1d2s configurations [16] and the relationship with the cluster and three-body continuum models which have been used for ^{11}Li [19].

a. Department of Physics, Faculty of Science, University of Tokyo, Hongo 7-3-1, Bunkyo-ku, Tokyo 113, Japan
b. Physics, Division, Argonne National Laboratory, Argonne, IL 60439-4843, USA

References

1. I. Talmi and I. Unna, Phys. Rev. Lett. **4** (1960) 469 .
2. S. Cohen and D. Kurath, Nucl. Phys. **73** (1965) 1.
3. D. J. Millener and D. Kurath, Nucl. Phys. **A255** (1975) 315.

4. D. J. Millener, J. W. Olness, E. K. Warburton and S. S. Hanna, Phys. Rev. **C28** (1983) 497.
5. A. G. M. van Hees and P. W. M. Glaudemans, Z. Phys. **A314**, 323 (1983); Z. Phys. **A315** (1984) 223.
6. T. Hoshino, H. Sagawa and A. Arima, Nucl. Phys. **A506** (1990) 271.
7. E. K. Warburton and B. A. Brown, Phys. Rev. **C46** (1992) 923.
8. T. Otsuka, N. Fukunishi and H. Sagawa, Phys. Rev. Lett. (1993) in press.
9. H. Kitagawa and H. Sagawa, Nucl. Phys. **A551** (1993) 16.
10. Nguyen van Giai and H. Sagawa, Phys. Lett. **106B** (1981) 379.
11. A. Bohr and B. R. Mottelson, Nuclear Structure Vol. 2 (W. A. Benjamin.,Inc., 1975) p. 221.
12. I. Ragnarsson, S. Aberg, H. B. Hakansson and R. K. Sheline, Nucl. Phys. **A361** (1981) 1. I. Ragnarsson, Proceedings of the Workshop on "the Science of Intense Radioactive Ion beams" (Los Alamos, LA-11964-c, April, 1990) p.199.
13. M. Fukuda, T. Ichihara, N. Inabe, T. Kubo, H. Kumagai, T. Nakagawa, I. Tanihata, Y. Yano, M. Adachi, M. Kouguchi, M. Ishihara, H. Sagawa and S. Shimoura, Phys. Lett. **B268** (1991) 339.
14. D. Kurath, Phys. Rev. Lett. **35** (1975) 1546.
15. A. Bohr and B. R. Mottelson, Nuclear Structure Vol. 2 (W. A. Benjamin.,Inc., 1975) p. 417.
16. F. C. Barker, J. Phys. **G2** (1976) L45.
17. E. K. Warburton, J. A. Becker and B. A. Brown, Phys. Rev. **C41** (1990) 1147.
18. J. L. Wood, K. Heyde, W. Nazarewicz, M. Huyse and P. van Duppen, Phys. Rep. **215**(1992) 101.
19. G. F. Bertsch and H. Esbensen, Ann. of Phys. **209** (1991) 327; H. Esbensen and G. F. Bertsch, Nucl. Phys. **A542** (1992) 310.

NATURE OF THE ^{20}Na 2646 keV LEVEL AND THE STELLER REACTION RATE FOR ^{19}Ne(p,γ)

B.A. Brown, A. E. Champagne[a], H.T. Fortune[b], and R. Sherr[c]

The region of excitation energy just above 2.2 MeV in ^{20}Na is important because of the possibility of a resonance in the astrophysically interesting [1] reaction ^{19}Ne(p,γ). Above the ^{19}Ne + p threshold at 2199 keV, the first known state [2-5] is at 2646 keV. This state is strongly populated [2,3] in ^{20}Ne(^{3}He,t)^{20}Na and has been variously incorrectly identified [2,3] as the mirror of the 3173- and 3448-keV 1^+ states in ^{20}F, and even [6] as the mirror of a supposed 1^- state at 3173 keV in ^{20}F.

Despite the large Coulomb shifts observed and expected for states containing significant $2s\frac{1}{2}$ strength, the 3448-keV 1^+ state is too far away for ^{20}Na (2646) to be its mirror. On the other hand, the ^{20}Na (3006) has a reasonable Coulomb shift and has been assigned 1^+ in the beta-delayed proton decay of ^{20}Mg [7] and is probably the analog of the ^{20}F (3448) state.

The 3173-keV state is probably [8] 1^+ and most likely [8] has a six-particle two-hole (6p-2h) configuration, i.e. $(sd)^6_{01}(1p)^{-2}_{10}$ (where subscripts denote angular momentum J and isospin T). This state would not be strong in ^{20}Ne(^{3}He,t); indeed in the mirror reaction [9] ^{20}Ne(t,^{3}He), ^{20}F (3173) is quite weak. It is very weak in all reactions [8,10-14], lending further support to its low J and core-excited nature [7]. A state of this configuration should have a negligible Coulomb shift, another reason why ^{20}Na (2646) is not its mirror. Remaining known candidates in ^{20}F are [5] a 3^+ state at 2966 keV and probable (3^-) and (4^-) states at 2865 and 2968 keV, respectively. With the exception of 0^- and 1^- states arising from coupling of a $p\frac{1}{2}$ hole to the $\frac{1}{2}^+$ excited state of ^{21}Ne (and ^{21}Na), other negative-parity states should have negligible Coulomb shifts. In fact, they should be slightly negative, with states in ^{20}Na lying somewhat higher than their ^{20}F counterparts. This expectation is borne out by the 2^- and 3^- states at 1309 (1338) and 1971 (1993) keV, respectively, in ^{20}F(^{20}Na). It is likely that the 996-keV level of ^{20}Na contains mirrors of both 984 keV, 1^- and 1057 keV, 1^+ states of ^{20}F. Similarly, the three states of ^{20}Na at 1841, 1993, and 2064 keV probably contain mirrors of five ^{20}F levels: 1824 keV, 5^+; 1844, 2^-; 1971, 3^-; 2044, 2^+; and 2194 keV, 3^+.

Finally, no states above 3.5 MeV in ^{20}F could correspond to ^{20}Na (2646), because the Coulomb shifts would be too large. By the process of elimination, then (assuming no states remain to be identified below 3.5 MeV in ^{20}F) the only ^{20}F state whose mirror could be ^{20}Na (2646) is the 3^+ at 2966 keV. With this identification the (t,^{3}He) and (^{3}He,t) cross sections are consistent and the Coulomb energy shift is appropriate. Hence, in what follows we take this assignment as determined, viz. J^π (2646) = 3^+.

To compute quantities of astrophysical interest, we need to know the proton and gamma widths of this state. For the proton width, a 3^+ couples to ^{19}Ne ($\frac{1}{2}^+$, gs) via $1d\frac{5}{2}$, and to ^{19}Ne ($\frac{5}{2}^+$, 238 keV) via $2s\frac{1}{2}$. Proton single-particle widths calculated with a Woods-Saxon potential (r_0 = 1.26, a = 0.60 fm) are $\Gamma_{sp}(p_0)$ = 9.7 eV and $\Gamma_{sp}(p_1)$ = 2.1 eV. The $\ell = 2$ spectroscopic factor for ^{20}F (2966) has been measured [12,15] in ^{19}F(d,p) to be 0.054. The shell-model value is 0.068. For ^{19}Ne* + $2s\frac{1}{2}$ we take the shell-model value of 0.347. Thus, proton widths are Γ_{p0} = 0.66 eV, Γ_{p1} = 0.73 eV.

Nothing is known of the γ decays of ^{20}Na (2646). Its mirror, ^{20}F (2966), has a mean life [5] of 60 $\pm$ 40 fs, decaying primarily via M1's to 2^+_1, 3^+_1, and 4^+_1 levels. The shell-model mean life for this ^{20}F state is 3.5 fs (see Table I), more than an order of magnitude shorter than the measured value, but consistent within the experimental uncertainty. [One prediction of the current work is that if the ^{20}F (2966) lifetime were to be better measured, a much smaller value should result.] Correcting for the E^3_γ factor and applying a small N, Z correction

in the M1 operator [16] the mean life in ^{20}Na should be 5.5 fs, i.e. $\Gamma_\gamma = 0.12$ eV. The decay properties of ^{20}Na (2646 keV, 3^+) are summarized in Table II.

Explosive hydrogen burning, which accompanies supernovae and powers cataclysmic binaries, is expected to proceed via the Hot CNO cycles or, for heavier nuclei, through the rp-process [1,17,18]. The former is considered to be the energy source for novae whereas the latter is thought to power more energetic explosions (e.g. x-ray bursts). An rp-process may be triggered directly from pre-existing A $\geq$ 20 nuclei or from lighter nuclei via several "breakout" reactions from the Hot CNO cycles. The link between the Hot CNO cycles and the rp-process is provided primarily by the ^{15}O(p,γ)^{19}Ne reaction [19] and to a lesser extent by the ^{18}F(p,γ)^{19}Ne and ^{18}N(α,p)^{21}Na reactions. Following either of the first two reactions, and rp-process may be initiated by a subsequent ^{19}N(p,γ)^{20}Na reaction. This reaction, like many in the rp-process, involves a short-lived nucleus (in this case $T_{1/2}$=17.2 s) and as a result, it has not been measured directly.

The quantity of interest for astrophysical applications is the thermonuclear reaction rate

$$< \sigma v >= \sqrt{(8/\pi\mu)}\,(kT)^{-3/2} \int \sigma(E)\, E \exp(-E/kT)$$

where μ is the reduced mass and k is the Boltzmann constant. In general, the cross section $\sigma(E)$ contains contributions from resonant and nonresonant processes. For an isolated narrow resonance at a center-of-mass energy E_{cm}, this expression reduces to

$$< \sigma v >= (2\pi/\mu kT)^{3/2}\, \hbar^2\, \omega\gamma \exp(-E_{cm}/kT)$$

For a (p,γ) resonance, the resonance strength $\omega\gamma$ is given by

$$\omega\gamma = \frac{(2J_f+1)}{2(2J_i+1)} \frac{\Gamma_p \Gamma_\gamma}{\Gamma}$$

Here J_f, and J_i are the spins of the final state and initial state, respectively, while Γ_p, Γ_γ, and Γ are the proton partial width, the γ-ray partial width, and total width of the resonance, respectively. Although the ^{19}N(p,γ)^{20}Na reaction has not been measured directly, it is possible to estimate resonance strengths using the structure of the A=20 nuclei as a guide. For example, proton widths can be obtained from the measured neutron spectroscopic factors of the mirror states in ^{20}F.

Breakout from the Hot CNO cycles is expected to occur for temperatures T > 0.4 x 10^9 K (or T_9 > 0.4) and densities in excess of $\rho = 10^3$ g/cm^3. These temperatures correspond to (most effective) energies in the ^{19}Ne + p system of E_{cm} > 185 keV. The properties of the first excited level above threshold at 2646-keV have been discussed above.

The 2857-keV state appears to correspond to the 2865-keV state in ^{20}F [$J^\pi = (3^-)$]. An $\ell = 3$ spectroscopic factor of (2J + 1)S = 0.044 has been measured [12,15] for the latter state via the ^{19}F(d,p)^{20}F reaction. This implies an f-wave proton width in ^{20}Na of $\Gamma_p = 0.02$ eV. No lifetime has been reported for either state, but an upper limit on the resonance strength can be obtained by assuming $\Gamma_\gamma = \Gamma_p$.

The 2986-keV state would be analogous to the $J^\pi = (4^-)$ state at $E_x = 2968$ keV in ^{20}F. Unfortunately, the latter state has not been resolved in the (d,p) reaction. However, because this state is apparently not a strong single-particle state and because its mirror would be an f-wave resonance (with a significant centrifugal barrier), it is unlikely that this resonance would have astrophysical importance.

TABLE I. Expected M1 decays of ^{20}F (2966) and ^{20}Na (2646), from shell-model calculations[a].

	^{20}F				^{20}Na			
J_f^π	$E_f^{(MeV)}$	$E_\gamma^{(MeV)}$	B(M1)	τ(fs)	E_f	E_γ	B(M1)	τ(fs)
2_1^+	0.0	2.966	0.285	7.6	0.0	2.646	0.300	10.2
3_1^+	0.656	2.310	0.160	28.7	0.606	2.040	0.181	36.9
4_1^+	0.823	2.143	0.676	8.5	0.808	1.838	0.523	17.5
Total				3.5				5.5

[a] The wave functions and effective operators used for the M1 matrix elements are described in Ref. 16. The E2 contributions are too small to cause appreciable changes.

For reactions involving ^{19}Ne in its *ground state*, the rate is dominated by the 447-keV resonance (Ex=2646 keV). However, by T_9=1, ^{19}Ne will be in its first excited state 15 percent of the time and in its second-excited state 3 percent of the time. For T_9 >2, the ground-state population falls below 50 percent of the total. Consequently, it is necessary to estimate the (p,γ) rate for reactions involving excited states of ^{19}Ne. We have discussed above the calculated Γ_p for populating the 2646-keV state from the first-excited state. The other resonances have strengths which appear to be determined primarily by the exit channel (i.e. $\omega\gamma \equiv \omega\Gamma_\gamma$) and as a result, they should not change dramatically with temperature unless the proton width is drastically decreased. Assuming that these latter strengths are in fact unchanged by thermal excitation in ^{19}Ne, an approximate analytic expression for the reaction rate which includes the effects of thermal excitation to the first-excited state (for population of the 2646-keV state) is

$$N_A < \sigma v >= 8.43\text{x}10^4\ (0.30+T_9^{-1.43}+T_9^{0.019})T_9^{-1.49}\ \exp(-5.516/T_9)\ \text{cm}^3\ \text{s}^{-1}\ \text{mole}^{-1}.$$

This approximation reproduces a more exact calculation to better than 20 percent over the temperature range $0.2 \leq T_9 \leq 2.0$ and once again the 2646-keV state is the major contributor to the total rate. For temperatures below this range, it is necessary to also include the direct-capture rate. Above $T_9 \equiv 2$, the population of higher-lying excited states cannot be ignored and so this approximation may not be accurate.

With our new calculations, the rate of the ^{19}Ne(p,γ)^{20}Na reaction is increased by about an order of magnitude over earlier results [2,3,4]. However, this increase is not astrophysically significant because the flow into the rp-process is limited by the rate of the (slower) ^{15}O(α,γ)^{19}Ne reaction. For T_9 = 0.4–2, the (p,γ) rate is 6.3-2.4 orders of magnitude greater than the (α,γ) rate (independent of density). In other words, once material is converted into ^{19}Ne, it will be rapidly passed along to higher masses.

TABLE II. Summary of widths for ^{20}Na (2646 keV, 3^+).

Channel	E_p (keV)	nlj	Γ_{sp} (eV)	S[a]	Γ (eV)
p_0	447	1d5/2	9.7	0.068	0.66
p_1	209	$2s\frac{1}{2}$	2.1	0.347	0.73
$\Sigma\gamma^{a,b}$		M1			0.12
Γ_{TOTAL}					1.51

[a] from shell model
[b] See Table I

Experimental verification of our results for the 2646-keV state are desirable and here the increased resonance strength is significant because it leads directly to a corresponding increase in the expected count rate for the ^{1}H(^{19}Ne,^{20}Na)γ reaction. Assuming a beam intensity of 1 pnA, the 2646-keV state will be produced at a

rate of 3860/hr. In addition, our predictions of $J^\pi = 3^+$ and $\Gamma_\gamma/\Gamma = 0.08$ can be examined via indirect nuclear spectroscopy. Such studies are in progress.

a. Department of Physics and Astronomy, University of North Carolina at Chapel Hill, North Carolina, 27599 and Triangle Universities Nuclear Laboratory, Duke University, North Carolina 27706
b. Physics Department, Univ. of Pennsylvania, 209 S 33rd St., Philadelphia, PA 19104
c. Physics Department, Princeton Univ., Princeton, NJ 08540

References

1. R. K. Wallace and S. E. Woosley, Astrophys. J. Suppl. **45**,389(1981).
2. L. O. Lamm, C. P. Browne, J. Görres, S. M. Groff, M. Wiescher, A. A. Rollefson, and B. A. Brown, Nucl. Phys. **A510**, 503 (1990); L. O. Lamm, C. P. Browne, J. Görres, M. Wiescher, and A. A. Rollefson, Z. Phys. A **327**, 239 (1987).
3. S. Kubono, *et al.*, Z. Phys. A **331**, 359 (1988); Astrophys. J. **344**, 460 (1989).
4. M. S. Smith, P. V. Magnus, K. J. Hahn, A. J. Howard, P. D. Parker, A. E. Champagne, and Z. Q. Mao, Nucl. Phys. A **536**, 333 (1992).
5. F. Ajzenberg-Selove, Nucl. Phys. A **475**, 1 (1987).
6. P. Descouvemont and D. Baye, Nucl. Phys. A. **517**, 143 (1990).
7. J. Gorres *et al.* , Phys. Rev. C **46**, R833 (1992); A. Piechaczek et al., Proceedings of the 6th International Conference on Nuclei far from Stability, Bernkastel-Kues, Germany, July 19-24, 1992, to be published.
8. R. Medoff, L. R. Medsker, S. C. Headley, and H. T. Fortune, Phys. Rev. C **14**, 1 (1976).
9. N. M. Clarke, *et al.*, J. Phys. G. **16**, 1547 (1990).
10. H. T. Fortune and J. N. Bishop, Nucl. Phys. A **293**, 221 (1977).
11. H. T. Fortune and J. D. Garrett, Phys. Rev. C **14**, 1695 (1976).
12. H. T. Fortune and R. R. Betts, Phys. Rev. C **10**, 1292 (1974).
13. G.-B. Liu and H. T. Fortune, Phys. Rev. C **37** , 1818 (1988).
14. G.-B. Liu and H. T. Fortune, Phys. Rev. C **38**, 2134 (1988).
15. H. T. Fortune, G. C. Morrison, R. C. Bearse, J. L. Yntema, and B. H. Wildenthal, Phys. Rev. C **6**, 21 (1972).
16. B. A. Brown and B. H. Wildenthal, Nucl. Phys. **A474** , 290 (1987).
17. M. Wiescher, J. Gorres, F.-K. Thielemann and H. Ritter, Astron. Astrophys.**160** , 56 (1986).
18. A. E. Champagne and M. Wiescher, Annu. Rev. Nucl. Part. Sci. **42** , 39 (1992).
19. P. V. Magnus, M. S. Smith, A. J. Howard, P. D. Parker and A. E. Champagne, Nucl. Phys. **A506** , 332 (1990).
20. K. Langanke, M. Wiescher, W. A. Fowler and J. Gorres, Astrophys. J. **301** , 629 (1986).
21. F. Ajzenberg-Selove, Nucl. Pys. **A475** , 1 (1987)

PARTICLE-ROTOR MODEL FOR N=7 NUCLEI

H. Esbensen[a], H. Sagawa[b] and B. A. Brown

Our shell-model studies of the parity inversion in ^{11}Be suggests that the even parity spectra of N=7 isotones may be described in terms of a simple neutron-core Hamiltonian, which includes a quadrupole nuclear coupling between the valence neutron and a deformed core. The odd parity spectra, on the other hand, are affected by the pairing blocking, and such a simple model would therefore not apply.

We have developed such a model Hamiltonian, with a quadrupole coupling strength that is consistent with the measured B(E2) values. The model describes the low-lying positive parity states in ^{11}Be and ^{13}C rather well. The ^{13}C spectrum is consistent with an oblate deformation of the core, whereas the ^{11}Be spectrum favors a prolate deformation. The $1/2^+$ ground state wave function that we obtain for ^{11}Be consists mainly of an $s_{1/2}$ single-particle state coupled to the 0^+ ground state of the core (80%), and a $d_{5/2}$ state coupled to the excited 2^+ core state (16%), consistent with the measured spectroscopic factor and shell-model calculations.

The simplicity of the model is very attractive and makes it easy to apply it and make comparisons to reaction data. An example is the angular distribution of neutrons emitted in ^{11}Be $\rightarrow$ ^{10}Be+n breakup reactions, which has recently been measured at GANIL. Coulomb dissociation dominates the breakup reaction on a gold target, and the model reproduces, in this case, both the shape and the absolute magnitude of the measured distribution.

a. Physics Division, Argonne National Laboratory, Argonne, IL 60439.
b. University of Tokyo, Hongo 7-3-1, Bunkyo-ku, Tokyo 113, Japan.

MOMENTUM DISTRIBUTIONS FOR (^{11}Li,^{9}Li+n+n) 3-BODY BREAKUP REACTIONS

H. Esbensen[a], G. F. Bertsch[b] and K. Ieki

The first coincidence measurements of the three-body breakup reaction, ^{11}Li $\rightarrow$ ^{9}Li+n+n, have now been analyzed[1]. The data were obtained at Michigan State University at a beam energy of 28 MeV/u on a lead target, and they provide the most detailed test of our three-body model[2,3] for ^{11}Li. Coulomb dissociation dominates the breakup reaction on the heavy target, and our comparisons to the data are based on this reaction mechanism. The new data show that the average velocity of the ^{9}Li fragments is larger than that of the emitted neutrons. This has been ascribed to a post Coulomb acceleration effect on the heavy fragment, when the breakup takes place in close vicinity of the target nucleus. This effect will also generate fluctuations in the velocity of the ^{9}Li fragment, and it is therefore experimentally difficult (event by event) to determine the momenta of the three emitted particles in the rest frame of the excited ^{11}Li nucleus.

Our calculated momentum distribution for the relative motion of the two emitted neutrons is in remarkably good agreement with the data. The recoil momentum distribution of the ^{9}Li fragment, on the other hand, is shifted to higher momenta compared to our prediction. This is illustrated in Fig. 1.

The measured decay energy spectrum, and the extracted dipole strength distribution are also shifted towards higher excitations compared to our predictions. These shifts are most likely due to the fluctuations generated by the post acceleration effect discussed above, whereas the momentum distribution for the relative motion of the two emitted neutrons is insensitive to this effect. In order to resolve the discrepancies with the data it is clearly necessary to include the post acceleration effect in the calculation. This will require a more detailed study or modeling of the decay of the excited ^{11}Li nucleus.

a. Physics Division, Argonne National Laboratory, Argonne, IL 60439.
b. Inst. of Nuclear Theory, Univ. of Washington, Seattle WA 98195.

References

1. 1. K. Ieki et al., Phys. Rev. Lett. 70, 730 (1993); D. Sackett et al., to be published.
2. 2. G. F. Bertsch and H. Esbensen, Ann. Phys. 209, 327 (1991).
3. 3. H. Esbensen and G. F. Bertsch, Nucl. Phys. A542, 310 (1992).

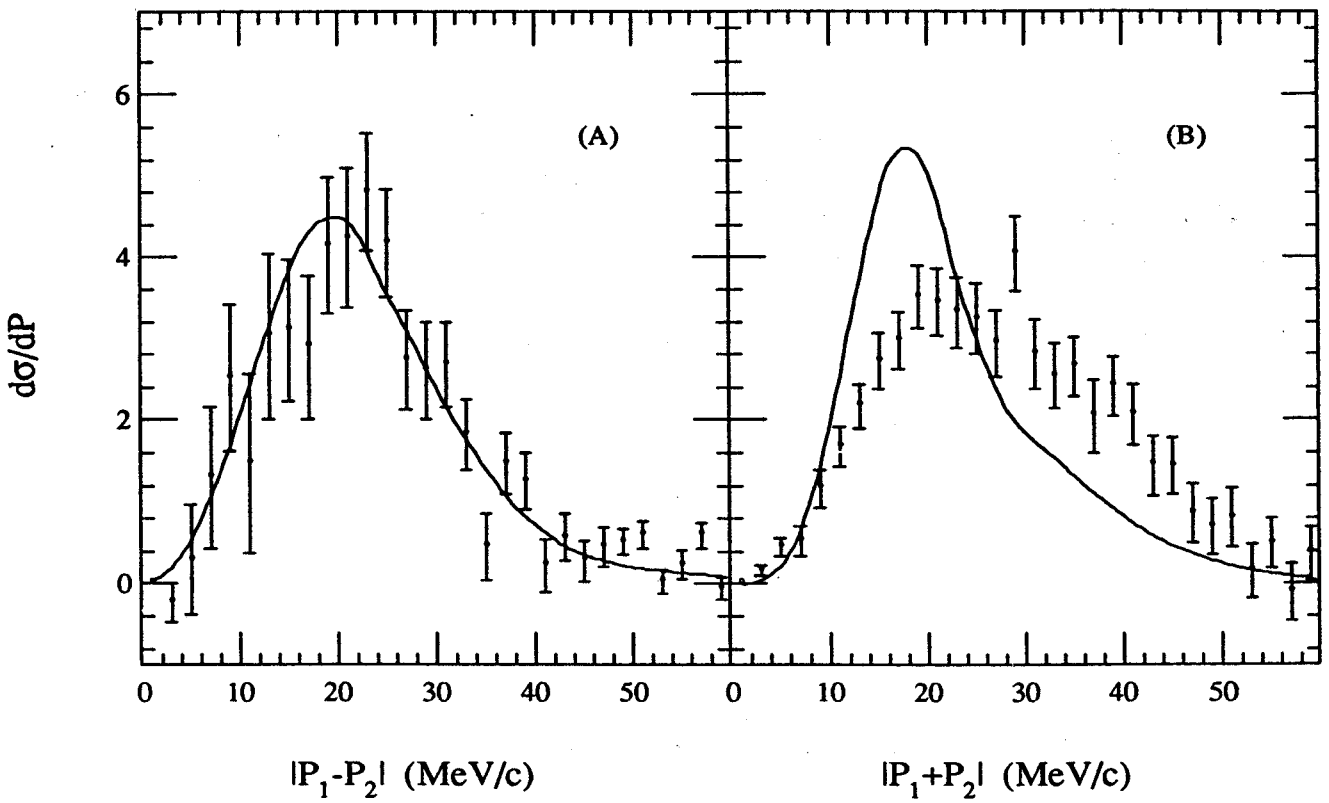

Figure 1: Momentum distributions for the relative motion of the two neutrons (a) and for the ^{9}Li recoil (b) in the rest frame of the ^{11}Li $\rightarrow$ ^{9}Li+n+n breakup reaction on a lead target at 28 MeV/u. The data are from Ref. 1. The calculated curves (normalized to 100) include the detection efficiency.

ALPHA DECAY OF ^{16}O EXCITED STATES

M. Grigorescu, B. Alex Brown and O. Dumitrescu

The theoretical study of α decay has provided a basic test for our understanding of several fundamental quantum phenomena, such as tunneling through the potential barrier, the clusterization process [1] and weak interaction models [2]. However, in spite of the effort invested, a detailed description of the α particle emission in not yet available.

By contrast to the case of γ or β decay, where the changes in the nuclear structure are small and may be treated within perturbation theory, α decay represent the simplest case of a series including phenomena like the heavy cluster decays and fission, when the transition has dramatic effects, generating in fact two new nuclei. For the calculation of the decay rate, an alternative to the Fermi's Golden Rule in this case was provided by the semiclassical approximation, or later on by the R-matrix theory of nuclear reactions [3]. Following the original description of Gamow, within this theory the α - decay assumes two stages, consisting of the process of preformation (structure part), and the process of penetration through the barrier (reaction part) [4-5]. The microscopic description of preformation has a key role in the understanding of the decay process and requires a precise knowledge of the initial quantum state. To achieve this purpose the shell model description has been continuously improved considering the correct treatment of Pauli effects [6] of the proton-neutron interaction [7] or extending the space with cluster wave functions [8-9].

In the present work [10] the α decay widths of several excited states of ^{16}O are calculated using the R-matrix formalism, with the shell-model wave functions given by three different interactions, ZBM-II [11] Z (ZWM) [12] and REWIL [13]. The model space considered (ZBM) is restricted to the last occupied level of ^{16}O $0p_{1/2}$ and the next two levels $0d_{5/2}$,$1s_{1/2}$ above the shell closure at N=Z=8. The structure of ^{16}O assumed here consists in an inert ^{12}C core, and four active nucleons. In the α decay these four nucleons are emitted, and the calculation of the widths provides a natural test of the effective interactions employed.

The ^{12}C - α scattering wave functions are generated by the Coulomb potential plus the realistic M3Y double folding potential [14] with Pauli corrections.

The main parameter of the R-matrix approach, the channel radius r_c is fixed near the last maximum r_f^{max} inside the Coulomb barrier for the radial function of the cluster component projected from the shell model state. To ensure the matching of the internal and scattering wave functions at r_c the nuclear folding potential $V_n(r)$ is renormalized to $(1+\varepsilon)V_n(r)$.

The comparison between the excitation energies and the decay widths obtained using REWIL (Table 1) and ZBM-II (Table 2) interactions shows that REWIL give better results for the 2^+ states, ZBM-II for the 0^+ states while in the case of the 4^+ transitions the quality is almost the same. In both cases the results indicate also a possible level crossing for the couple $4_3^+ - 4_4^+$ with respect to the data.

Table 1: Excitation energies (MeV), widths (KeV), and matching parameters for the states 0_i^+,2_i^+,4_i^+ obtained with the REWIL interaction

L_i^+	E^{exp}	E^{th}	Γ_{exp}	Γ_{th}	ε	r_c[fm]	r_f^{max}[fm]
0_2^+	11.26	11.6	(2500)?	903	5%	3.34	3.34
0_3^+	12.05	14.5	1.5±0.5	96	-15%	2.44	2.44
0_4^+	14.03	15.9	200±15	26	32%	3.79	3.79
2_2^+	9.84	9.66	0.625±0.1	1.1	0%	4.1	4.3
2_3^+	11.52	13.32	71±3	38.1	24.5%	4	4
2_4^+	13.02	14.99	150±10	245	14%	3.09	3.09
4_1^+	10.35	11.4	27±3	34.3	100%	3.43	3.43
4_2^+	11.09	13.3	0.28±0.05	0.7	0%	3.95	4.07
4_3^+	13.87	14.3	~49	293	29%	3.66	3.66
4_4^+	14.62	16.6	~389	36.2	30%	3.63	3.63

Table 2: Excitation energies (MeV), widths (KeV), and matching parameters for the states 0_i^+,2_i^+,4_i^+ obtained with the ZBM-II interaction

L_i^+	E^{exp}	E^{th}	Γ_{exp}	Γ_{th}	ε	r_c[fm]	r_f^{max}[fm]
0_2^+	11.26	10.73	(2500)?	502	13.8%	3.21	3.21
0_3^+	12.05	12.44	1.5±0.5	0.13	-22%	4.41	4.41
0_4^+	14.03	14.58	200±15	214	-5%	3.44	3.44
2_2^+	9.84	10.54	0.625±0.1	6.7	-30%	3.8	3.89
2_3^+	11.52	13.27	71±3	192	-14%	3.79	3.79
2_4^+	13.02	13.54	150±10	23.8	20%	4.19	4.19
4_1^+	10.35	10.42	27±3	26	90%	3.41	3.41
4_2^+	11.09	13.58	0.28±0.05	3.5	-30%	3.6	3.7
4_3^+	13.87	14.54	~49	709	-8.5%	3.2	3.2
4_4^+	14.62	15.60	~389	0.06	-2%	3.14	3.14

The calculated widths are in a reasonable agreement with experiment, reproducing quite well the variations of several orders of magnitude observed between the decay widths for the low-lying 0^+, 2^+ and 4^+ states. The remaining differences may be due to the limitations of the model space, as well as to possible inversions in the level ordering. However this shell-model treatment proves to reproduce a large amount of experimental data in ^{16}O, indicating the relevance of the present attempt to achieve a microscopic description of the α decay.

References

1. Y. Akaishi, K. Kato, H. Noto, S. Okabe, Developements of Nuclear Cluster Dynamics, World Scientific Publishing Co. Pte. Ltd. 1989
2. M. Gari, Phys. Reports **6 C** (1973) 317
3. A.M.Lane and R.G.Thomas, Rev. Mod. Phys. **30** (1958) 257
4. H.J. Mang, Ann. Rev. Nucl. Sci. **14** (1964) 1; Z. Phys. **148** (1957) 572; Phys.Rev. **119** (1960) 1069
5. O. Dumitrescu, Fiz. Elem. Chastits At. Yadra 10(1979)377 (Sov.J. Part. Nucl. **10** (1979) 147)
6. A. Bulgac, S. Holan, F. Carstoiu and O. Dumitrescu, Nuovo Cimento **70 A** (1982) 142
7. G. Dodig-Crnkovic, F.A. Janouch, R.J. Liotta, Nucl. Phys.**A 501** (1989) 533
8. T. Tomoda, A.Arima, Nucl. Phys.**A 303** (1978) 217
9. K. Varga, R.G. Lovas, R.J. Liotta, Nucl. Phys.**A 550** (1992) 421
10. M. Grigorescu, B. Alex Brown, O. Dumitrescu, submitted to Phys. Rev. C
11. A.P. Zuker, B. Buck, J.B. McGrory, Phys. Rev. Lett. **21** (1968) 39
12. A.P. Zuker, Phys. Rev. Lett. **23** (1969) 983
13. B.S. Reehal, B.H. Wildenthal, Part. and Nucl. **6** (1973) 137
14. G. Bertsch, J. Borisowicz, H. McManus and W.G. Love, Nucl. Phys. **A 284** (1977) 399

HEAVY ION CHARGE EXCHANGE IN THE EIKONAL APPROXIMATION

C. A. Bertulani

In high-energy collisions (E_{lab} > 50 MeV/nucleon) the eikonal approximation provides a transparent description of heavy ion charge exchange reactions. The formalism is applied to the reaction $^{13}N(^{13}C, ^{13}N)^{13}C$ at 70 MeV/nucleon. The relative contributions of pion- and rho-exchange are determined. It is found that heavy ion reactions are more sensitive to the one-pion exchange component of the interaction than nucleon-induced charge exchange. The cross section for double charge exchange are estimated, which could be useful for future experiments.

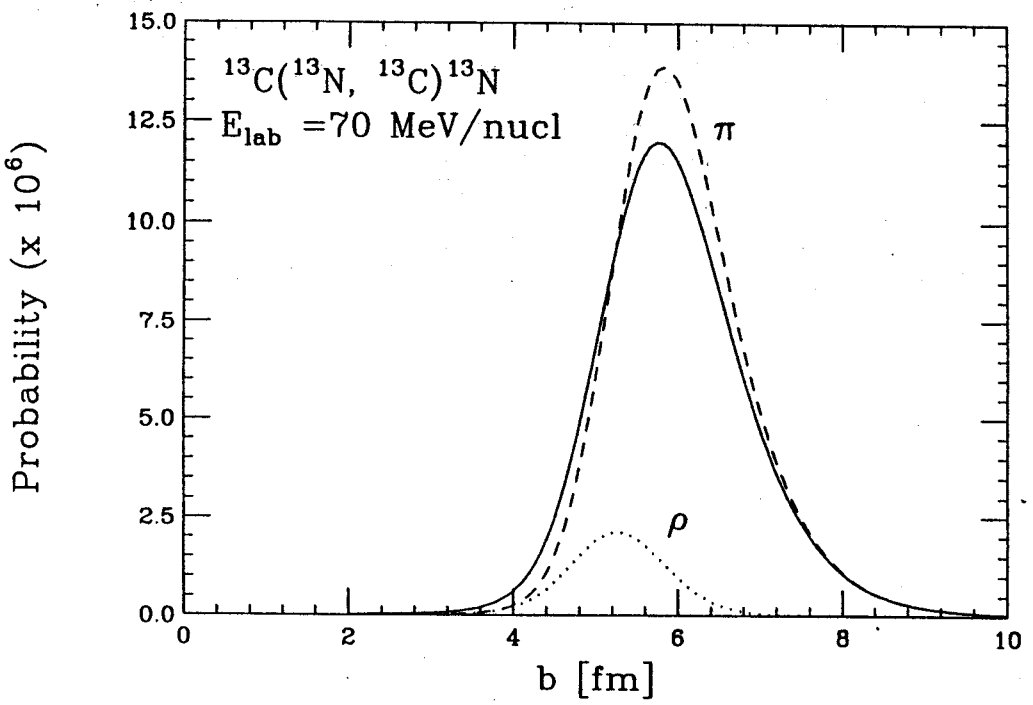

Figure 1: Probability for π- (dashed-curve) and ρ-exchange (dotted-curve) in the reaction $^{13}C(^{13}N, ^{13}C)^{13}N$ at 70 MeV/nucleon, as a function of the impact parameter. The solid curve represents the result of the full interaction.

Figure 1 shows the contributions from π (dashed-curve) and from ρ-exchange (dotted-curve) to the charge exchange probability as a function of the impact parameter. The solid curve is the total probability. The exchange probability is peaked at grazing impact parameters: at low impact parameters the strong absorption makes the probability small, whereas at large impact parameters it is small because of the short-range of the exchange potentials. The value of the exchange probability at the peak is about 1.2×10^{-5}. It is clear from figure 1 that the process is dominated by π-exchange. At small impact parameters the short-range ρ-exchange contribution is large due to a larger overlap between the nuclei.

In Figure 2 the differential cross section is plotted. One observes that at very forward angles the π-exchange contributes to the largest part of the cross section. But ρ-exchange is important at large angles. It has the net effect of smoothing out the dips of the angular distribution. Since π-exchange is of longer range

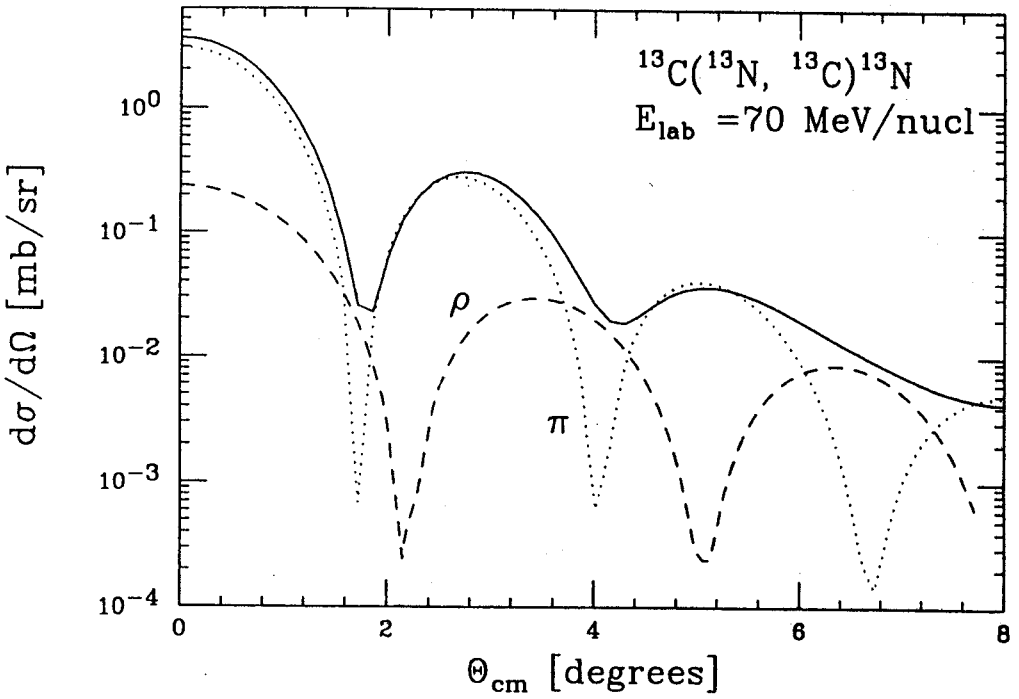

Figure 2: Angular distribution for charge-exchange in the reaction $^{13}C(^{13}N, ^{13}C)^{13}N$ at 70 MeV/nucleon. The contribution from π- (dashed-curve) and ρ-exchange (dotted-curve) are displayed separately. The solid curve represents the result of the full interaction.

than ρ-exchange, the dips caused by the two contributions are displaced; the ones from ρ-exchange alone are located at larger angles, as expected from the relation $\theta \sim 1/r$. If we put $\mathcal{F}_{0,2} = 1$ and $\exp i\chi(b) = 1$, we obtain that at very small scattering angles the π- and ρ-exchange contributions to the differential cross sections are approximately of the same magnitude. This means that ρ-exchange is more important when distortions are weaker, i.e., in nucleon-nucleon or nucleon-nucleus scattering.

MOMENTUM DISTRIBUTIONS IN REACTIONS WITH RADIOACTIVE BEAMS

C. A. Bertulani and K.W. McVoy[a]

Fragmentation reactions with secondary beams of radioactive nuclei have shown that the total reaction cross sections and the transverse momentum distribution of the fragments are sensitive to the separation energy of the last neutrons and to the size of the density profile in these nuclei [1]. These two quantities are linked since the "size" of the nucleus is roughly proportional to the inverse of the square root of the separation energy. Using the Goldhaber model for soft fragmentation, the authors of ref. (1) were able to relate the widths of the narrow peaks in the transverse momentum distributions with the separation energies and sizes of the radioactive nuclei. However, this approach is not free of bias. The interaction of the fragments with the target broadens the narrow peak and makes the extraction of quantitative information about these quantities strongly model-dependent and potentially inaccurate.

We show here that a better measure of the interaction size of the radioactive projectile is obtained by the longitudinal momentum distribution of its fragments. It is also shown that the Coulomb and nuclear fragmentation amplitudes have longitudinal momentum distributions with very nearly equal widths. This fact has indeed been verified in a recent experiment at the NSCL/MSU [2]. On the other hand, the transverse momentum distributions are substantially broadened by the size and diffuseness of the region of overlap with the target and contain Coulomb and nuclear contributions with different widths. The interpretation of the "wide" (core-neutron) component of the transverse momentum distributions is therefore less straightforward than is that of the longitudinal ones [3].

a. Physics Department, University of Wisconsin, Madison, Wisconsin 53706, USA

References

1. T. Kobayashi *et al.*, Phys. Rev. Lett. **60** (1988) 2599;T. Kobayashi, I. Tanihata, Proc. Int. Symposium on Structure and Reactions of Unstable Nuclei, June 17-19, 1991, Niigata, Japan, World Scientific, ed. by T. Suzuki.
2. N. Orr *et al.*, Phys. Rev. Lett. **69** (1992) 2050
3. C.A. Bertulani and K.W. McVoy, Phys. Rev. **C46** (1992) 2638

DIFFERENTIAL CROSS SECTIONS OF SOFT MULTIPOLE STATES

C.A. Bertulani and H. Sagawa[a]

We study the differential cross sections of the soft multipole excitations of ^{11}Li with C-target by using a reaction model in which all input parameters are determined from other sets of experimental data. The results describe properly the differential cross sections of giant resonances in ^{208}Pb excited by an α-projectile at an intermediate energy E_{lab}=43 MeV/u without introducing any free parameters (see fig. 1). Predicted cross

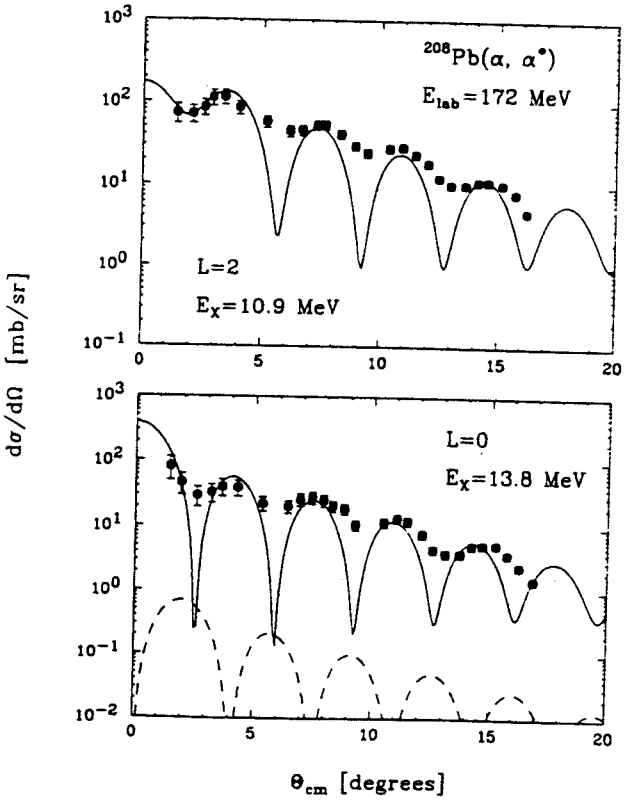

Figure 1

sections for soft multipole excitation are of the order of 100 mb/sr at forward angles in heavy ion reactions at beam energies in the range 30-70 MeV/nucleon (see fig. 2). It might be possible to distinguish the multipoles experimentally by the angular dependence at very forward angles.

a. Dept. of Physics, Faculty of Science, Univ. of Tokyo, Hongo 7-3-1, Bunkyo-ku, Tokyo 113, Japan

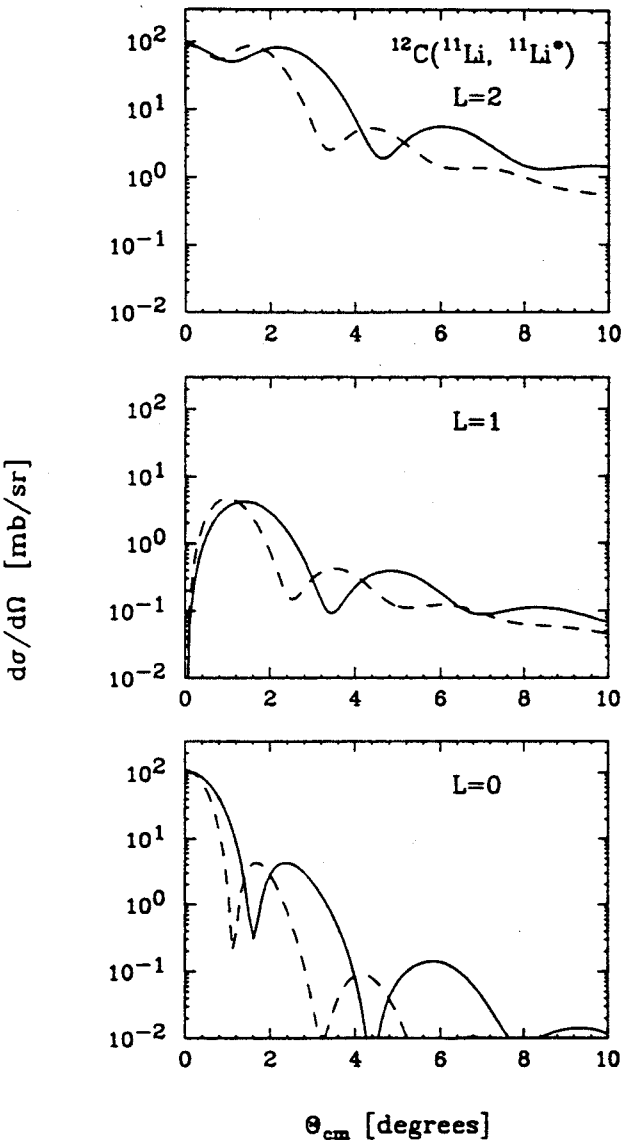

Figure 2

EXCITATION OF MULTIPHONON STATES IN RELATIVISTIC HEAVY ION COLLISIONS

C. A. Bertulani and V. Zelevinsky

We investigate the excitation of multiphonon states in relativistic heavy ion collisions. We use a semi-classical formalism to determine the one-step and two-step Coulomb excitation of the double-phonon GDR × GDR excitation. The excitation cross sections of the $L = 0$ state and of the $L = 2$ state are determined separately. The nuclear contributions to the process are also calculated. The key ingredients of our approach are (i) sum rules which are used to evaluate the multipole matrix elements for the first and second excitation steps and (ii) taking into account the widths of final and intermediate states. Physical problems related to the spreading width of the double phonon states are discussed in detail.

A comparison with recent experimental data[1] shows a good agreement. Some of our results are presented in the tables below.

	$m = \pm 2$	$m = \pm 1$	$m = 0$	σ_{total}	σ_{width}
IVGDR	-	712	201	1630	1820
ISGQR	64	6.09	10.6	150	169
IVGQR	25.6	5.46	12.4	74.5	97

Table I - Cross sections (in mb) for the Coulomb excitation of the IVGDR, ISGQR and IVGQR in ^{136}Xe incident on Pb at 0.69 GeV/nucleon. The contributions to the population of each angular momentum projections are shown separately. In the last column the total cross sections are calculated with the widths of the states taken into account.

Double-phonon state	$m = \pm 2$	$m = \pm 1$	$m = 0$	σ_{total}	σ_{width}
L=0 (two-step)	-	-	41	41	51
L=2 (two-step)	41.2	19.7	40.9	163	201
L=2 (direct – 20% of SR)	3.27	0.86	2.12	10.3	11.8

Table II - Cross sections (in mb) for the Coulomb excitation of the double-GDR, in ^{136}Xe incident on Pb at 0.69 GeV/nucleon. The contributions to the L=0 and the L=2 states are shown separately. In the last column the total cross sections are calculated with the widths of the states taken into account.

References

1. R. Schmidt et al., Phys. Rev. Lett. **70** (1993) 1767

COULOMB REACCELERATION AS A CLOCK FOR NUCLEAR REACTIONS

G. Bertsch and C. A. Bertulani

A possible measure of the time scale for projectile breakup reactions is the acceleration in the target Coulomb field following the excitation process. We model this by solving the time-dependent Schroedinger equation in one dimension, comparing with simple arguments based on the uncertainty principle. We find that momentum shifts are generally much larger than given by simple arguments based on classical mechanics and the uncertainty principle. Fig. 1 shows the net momentum of particles emitted from a square barrier potential under the influence of a Coulomb dipole interaction. Also shown is the free particle momentum (Coulomb deflection for a given impact parameter) and the prediction of a classical resonance model, where the breakup processes is assumed to take in three-steps: (a) excitation of the particle to the resonance, (b) time-delay due to the finite width of the resonance and (c) free reacceleration of the particle after it tunnels through the barrier.

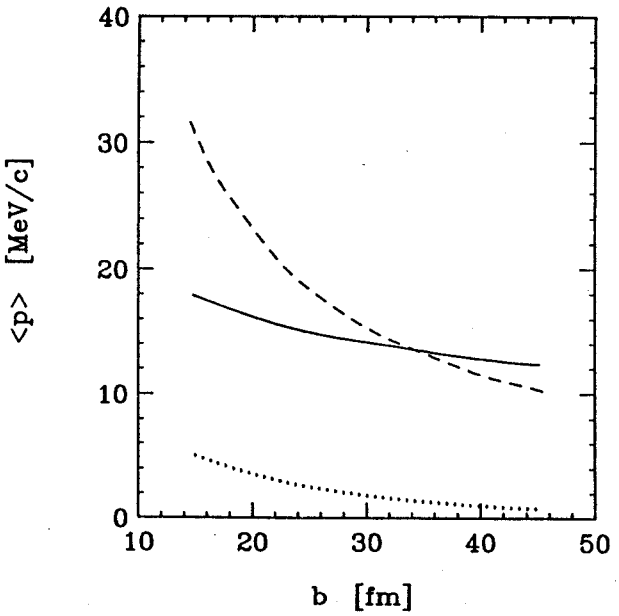

Figure 1: Momentum shift of the continuum particle excited from the square barrier potential, as a function of impact parameter in the collision (solid curve). The dashed curve is the momentum transfer in the instantaneous emission model and the dotted curve is the prediction from classical resonance decay.

Although there is some reduction of the momentum shift of the particle due to the finite time for barrier penetration, the momentum is far larger than in the resonance model. Obviously, the barrier penetration is strongly connected with the excitation process. In our model, the resonance is penetrated preferentially on one side where the barrier is lower. The qualitative behaviour of this result is independent of the strength of the exciting field, and is essentially reproducible in second-order perturbation theory. The net momentum per emitted particle is linear in the external field in second-order perturbation theory, just as the classical momentum.

Our results suggest that Coulomb acceleration is intrinsically quantum mechanical for conditions typical in light nuclei. One cannot approximate its effects by assuming that it only acts in the post-breakup phase of the reaction. The accelerations can be much larger, and experiments that use Coulomb breakup to measure

properties of the nucleus may be more problematic as a consequence of the more persistent acceleration. For example, this technique was used to infer the dipole excitation strength for the ^{6}Li $\rightarrow$ ^{4}He + d breakup in ref. (1).

In the breakup reaction ^{11}Li $\rightarrow$ ^{9}Li + neutrons, the neutrons were observed in a very narrow cone about the beam axis [2]. In our model, there would be essentially no transverse momentum transfer associated with the Coulomb trajectory of the Li projectile. This would help preserve the narrowness of the angular distribution in the laboratory frame, given a neutron momentum distribution predicted by first order perturbation theory.

Qualitatively, we did find a suppression of the postacceleration when the particle was excited to a narrow resonance. This clearly shows that the time delay in emitting the particle can play an important role, although one that does not seem to be easy to estimate.

However, we must emphasize again that these results were obtained for a greatly oversimplified model, putting all of the physics into one dimension. It would be much more realistic to study the three-dimensional Schroedinger equation. Then one can separately treat the excitation, which occurs dominantly in the transverse direction, and the reacceleration, which is observed in the longitudinal direction. It seems to us to be worthwhile to pursue this, in view of the potential importance of reacceleration both as a measuring tool and as an obscuring agent in the application of Coulomb breakup.

References

1. J. Kiener et al., Phys. Rev. C33 2195 (1991).
2. K. Ieki et al., Phys. Rev. Lett. **70** (1993) 730;

HIGHER-ORDER ELECTROMAGNETIC INTERACTION IN THE DISSOCIATION OF FAST PARTICLES

C. A. Bertulani, G. Baur[a] and D. Kalassa[a]

We investigate the effects of (Coulomb) post-acceleration in break-up process of light heavy ion reactions. These effects are of relevance if one wants to deduce the invariant mass of the excited nucleus. We study the case of the fragmentation of ^{11}Li projectiles in intermediate energy collisions. A classical and a semiclassical calculation are used for the purpose. In the figure below we show the extra-energy, i.e., the energy gained by the fragments due to their reacceleration in the Coulomb field of the target after the breakup. A semiclassical approach was used in the calculation.

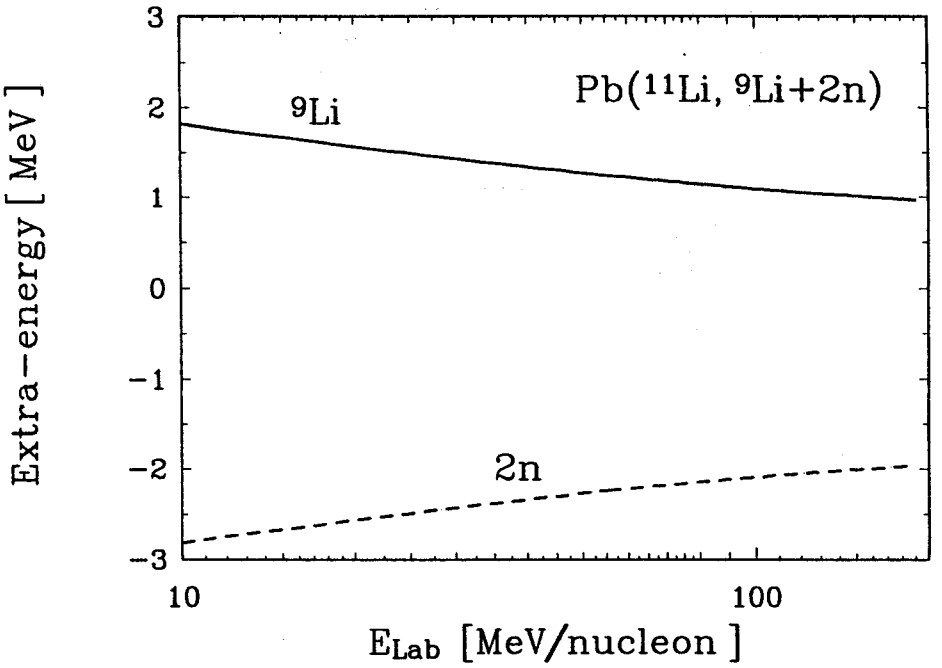

Figure 1: Post-acceleration energy of ^{9}Li fragments (solid) and the two neutrons (dashed) in the reaction $^{11}Li + ^{208}Pb$ as a function of the bombarding energy

a. Institut für Kernphysik, Forschungsanlage Jülich, Postfach 1913, 5170 Jülich, Germany

STRUCTURE AND REACTIONS OF NEUTRON-RICH NUCLEI

C.A. Bertulani, L.F. Canto[a] and M.S. Hussein[b]

We review the present status of the structure and reactions of neutron-rich nuclei. The properties of the low-lying soft giant resonance in ^{11}Li are discussed within several models proposed in the literature. The existence of this collective mode in heavier neutron-rich nuclei is considered. The question of the separation energy of a single neutron and a dineutron is discussed.

The nuclear and Coulomb dissociation cross sections for ^{11}Li on several targets are calculated and compared to the available data. The question of the neutron halo is considered in detail.

The elastic scattering of ^{11}Li and other unstable nuclei on several targets (p, ^{208}Pb, etc) is discussed in detail. The signature of the halo on the elastic cross section σ_{el} is then assessed. Proposed experiments are then discussed in light of the theoretical predictions. The effect of the break-up channel on σ_{el} is thoroughly analysed. The total reaction cross section and total nuclear reaction cross section is also calculated using the microscopic $t\rho_1\rho_2$-Glauber theory. The production of π's is considered and model calculations are performed.

The low-energy fusion of neutron-rich nuclei with heavy targets is analysed. Having in mind the possibility that the low-lying soft giant-resonance may greatly aid the system to fuse even at sub-barrier energies, the viability of producing superheavy elements will be studied. The astrophysical implications of exotic nuclei are assessed and discussed. Finally, the momentum and angular distributions of fragments from ^{11}Li breakup are calculated and compared to the available data.

a. Insituto de Física, Universidade Federal do Rio de Janeiro, 21945 Rio de Janeiro, RJ, Brazil
b. Insituto de Física, Universidade de São Paulo, 01498 São Paulo, SP, Brazil

MULTIPOLE RESPONSE OF ^{11}Li

C. A. Bertulani and A. Sustich[a]

We investigate the electric multipole response of ^{11}Li which could be tested in reactions with secondary beams at intermediate and high energies. We use simple arguments to show that, even in the most favorable cases, electric dipole excitations are by far dominant. The contributions from higher order multipolarities will be less than the presently attainable experimental uncertainties.

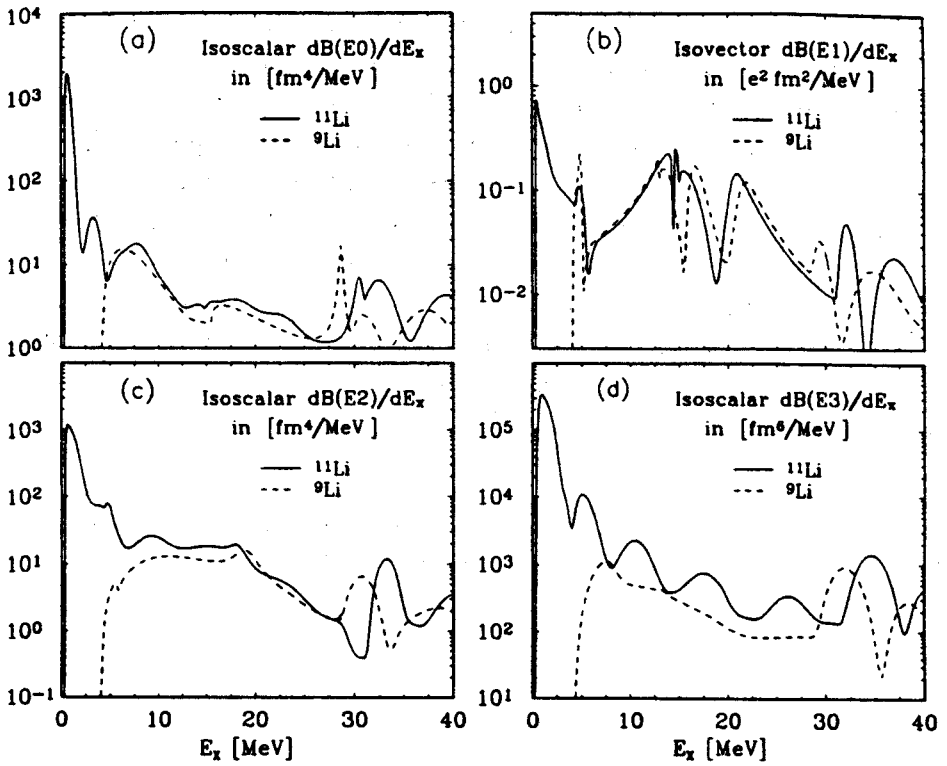

Figure 1: RPA response of ^{11}Li (solid) and ^{9}Li (dashed) for the a) isoscalar monopole, b) "isovector" dipole, c) isoscalar quadrupole, and the d) isoscalar octupole.

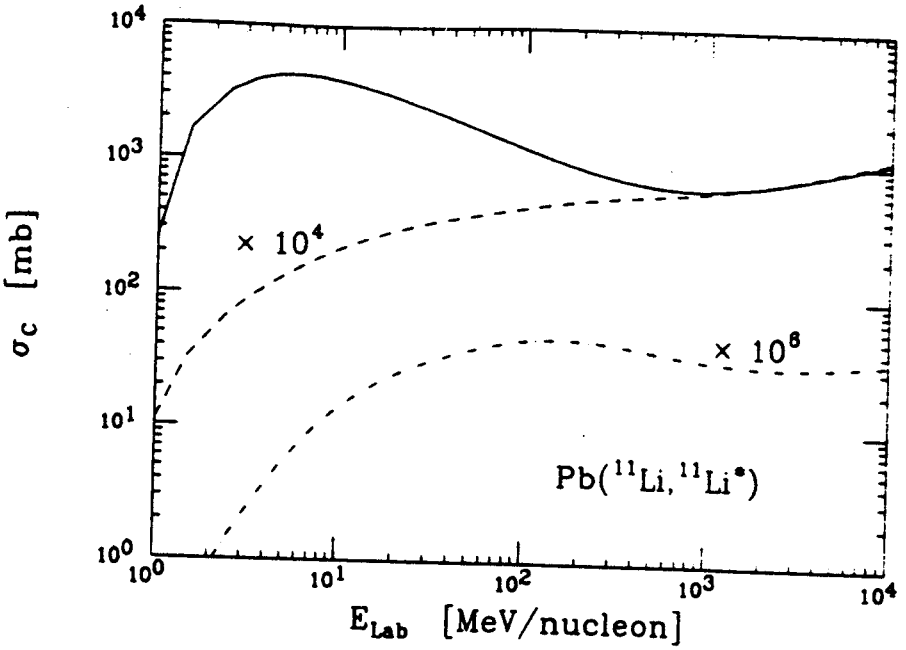

Figure 2: Total Coulomb excitation cross section of ^{11}Li projectiles incident on a lead target as a function of the beam energy. The solid (dashed) line represents the contribution of isovector dipole (effective-charge corrected quadrupole) excitations. The dashed-dotted line represents the contribution of effective-charge corrected octupole excitations. The quadrupole and the octupole results have been multiplied by 10^4 and 10^6, respectively.

a. Department of Computer Science, Mathematics and Physics, Arkansas State University, State University, AR 72467-0070